

# Chapter 2

## The Effect of Mechanical Activation on the Synthesis and Properties of Multiferroic Lead Iron Niobate

A. A. Gusev, I. P. Raevski, E. G. Avvakumov, V. P. Isupov,  
S. P. Kubrin, H. Chen, C.-C. Chou, D. A. Sarychev, V. V. Titov,  
A. M. Pugachev, S. I. Raevskaya and V. V. Stashenko

The present work studies the effect of high-energy mechanical activation using the planetary-centrifugal ball mill AGO-2 and subsequent annealing on the synthesis and magnetic properties of  $\text{PbFe}_{0.5}\text{Nb}_{0.5}\text{O}_3$  (PFN). This technique enables one to perform the mechanically activated synthesis of PFN at much shorter time. The results of X-ray phase analysis, electron microscopic studies and transmission Mössbauer  $^{57}\text{Fe}$  spectra measurement are presented and discussed. Mössbauer studies show that the temperature of magnetic phase transition in  $\text{PbFe}_{0.5}\text{Nb}_{0.5}\text{O}_3$  powders can be changed by mechanical activation and subsequent annealing.

### 2.1 Introduction

Lead iron niobate  $\text{PbFe}_{0.5}\text{Nb}_{0.5}\text{O}_3$  (PFN) is a ternary perovskite oxide possessing both ferroelectric (ferroelectric Curie temperature  $T_C \approx 380$  K) and magnetic (temperature of antiferromagnetic phase transition, i.e. Néel temperature,  $T_N \approx 150$  K) properties [1]. PFN is a promising basic material for multilayer

---

A. A. Gusev · E. G. Avvakumov · V. P. Isupov  
Institute of Solid State Chemistry and Mechanochemistry SB RAS, Novosibirsk, Russia

I. P. Raevski · S. P. Kubrin · D. A. Sarychev · V. V. Titov · S. I. Raevskaya (✉) ·  
V. V. Stashenko  
Research Institute of Physics and Physical Faculty, Southern Federal University,  
Rostov-on-Don, Russia  
e-mail: sveta.raevskaya@mail.ru

H. Chen  
University of Macau, Macau, China

C.-C. Chou  
National Taiwan University of Science and Technology, Taipei 10607,  
Republic of China (Taiwan)

A. M. Pugachev  
Institute of Automation and Electrometry, SB RAS, Novosibirsk, Russia

capacitors, pyroelectric sensors, piezoelectric ceramics and electrostrictive actuators [2–6]. It is also a component of some novel room-temperature multiferroic magnetoelectrics [7].

The temperature of magnetic phase transition in Fe-containing oxides is believed to depend on the number of possible Fe–O–Fe linkages in a crystal lattice [8]. In ternary  $\text{PbFe}_{0.5}\text{B}_{0.5}\text{O}_3$  perovskites this number can be governed, e.g. by changing the degree  $S$  of  $B$ -cation ordering, as the ordering changes the number of magnetic ions in the neighboring unit cells and thus reduces the possible number of Fe–O–Fe linkages. However in contrast to  $\text{PbB}^{3+}_{0.5}\text{B}^{5+}_{0.5}\text{O}_3$  perovskites with  $B^{3+} = \text{Sc}, \text{Yb}; B^{5+} = \text{Nb}, \text{Ta}$ , [9, 10], no superstructural reflections on X-ray diffraction patterns due to  $B$ -cation ordering have been reported for PFN [8, 11]. At the same time, the experimental value of  $T_N$ , for PFN ( $\approx 150$  K) is located approximately half-way between calculated values of this temperature for the fully ordered ( $T_N = 0$  K) and completely disordered ( $T_N \approx 400$  K) states [8]. This fact is usually interpreted as an evidence of a partial ordering of  $\text{Fe}^{3+}$  and  $\text{Nb}^{5+}$  cations [8]. The possible reason of the absence of superstructural reflections on X-ray diffraction patterns is a local character of ordering in PFN, i.e. mesoscopic domains of several nanometers in size with different values of  $S$  coexist in a crystal. Another evidence of the chemically inhomogeneous nature of PFN was obtained from the studies of magnetization [1, 11],  $^{93}\text{Nb}$  and  $^{17}\text{O}$  NMR [12] and Mössbauer  $^{57}\text{Fe}$  spectra [13], diffuse neutron scattering [11] as well as from the results of the first-principal calculations [13]. Long range AFM order seems to develop in Fe-rich-Nb-poor regions while, a short-range ordered spin-glass-like state can arise at low ( $T \approx 10\text{--}20$  K) temperatures from the Fe-poor-Nb-rich regions. AFM and spin-glass states can coexist in a wide temperature range [14]. Magnetic phase transition temperature in PFN is more than 100 K higher as compared to lead-free  $\text{AFe}_{0.5}\text{Nb}_{0.5}\text{O}_3$  ( $A = \text{Ca}, \text{Sr}, \text{Ba}$ ) perovskites [15, 16]. This dramatic difference is attributed to the possibility of magnetic super-exchange via an empty  $6p$  state of  $\text{Pb}^{2+}$  ions [15, 16] as well as for the clustering of iron ions in the lattice [13]. Both the degree of  $B$ -cation compositional ordering and clustering of iron ions are known to be influenced by mechanical activation, which has been successfully used for the synthesis and preparation of ternary lead-based perovskite ferroelectrics [17, 18]. This method enables one to obtain nanodispersed powders with high sintering ability thus lowering substantially the sintering temperature of ceramic materials. We have found in the literature two works devoted to the application of the mechanical activation method for synthesis of PFN [19, 20]. However, the effect of mechanical activation on magnetic properties of PFN has not been studied yet. Moreover, the energy of mechanical activation, used in [19, 20], was rather modest and the activation time varied from 20 to 30 h. Recently the planetary-centrifugal ball mill AGO-2 enabling activation with much higher energy than in [19, 20] was designed [17]. The aim of the present work was to study the effect of high-energy mechanical activation using AGO-2 mill and subsequent annealing on the synthesis and magnetic properties of PFN.

## 2.2 Experimental

In order to compare the effect of high-energy milling on PFN synthesis, two batches were used: stoichiometric mixture of PbO, Fe<sub>2</sub>O<sub>3</sub> and Nb<sub>2</sub>O<sub>5</sub> oxide powders (**I**) and stoichiometric mixture of PbO and preliminary synthesized FeNbO<sub>4</sub> precursor (**II**). The starting oxides were Nb<sub>2</sub>O<sub>5</sub> (the American Society for Testing Materials (ASTM) code 16-53, 37-1468), monoclinic modification, space group P2 (no. 3), OSCh reagent grade (high pure); Fe<sub>2</sub>O<sub>3</sub> (ASTM code 85-599) hematite, rhombohedral modification, space group R-3C (no. 167), ChDA reagent grade (pure for analysis); PbO (ASTM code 72-93) massicot, orthorhombic modification, space group Pbcm (no. 57), ChDA reagent grade (pure for analysis), with Pb<sub>3</sub>O<sub>4</sub> admixture (ASTM code 41-1493) minium, tetrahedral modification, space group P42/mbc (no. 135). The mechanical activation was carried out using the high-energy planetary-centrifugal ball mill AGO-2 under a ball acceleration of 40 g. A mixture of powdered reagents (10 g) was placed into steel cylinder together with 200 grams of steel balls 8 mm in diameter. Activation was carried out for 5, 10 and 15 min. After each 5 min of activation, the mill was stopped, the cylinders were opened, the powder was taken out and mixed then it was put back into the cylinders for further mechanical activation. The samples for subsequent annealing were pressed at 1000 kg/cm<sup>2</sup> without a plasticizer. Annealing of the samples, placed into a closed alumina crucible, was carried out in an electric oven at different temperatures for 2 h. Heating rate was 10 deg/min. The samples were cooled together with the furnace after it was switched off. X-ray phase analysis was performed using DRON-3 diffractometer and Cu-K<sub>α</sub> radiation. Electron microscopic studies were carried out with a transmission electron microscope (TEM) JEM-2000FX II (JEOL) at the accelerating voltage of 200 kV. Transmission Mössbauer <sup>57</sup>Fe spectra were measured with the aid of MS-1104EM rapid spectrometer and analyzed using the original computer program UNIVEM. The sample holder was attached to the closed-cycle helium cryostat-refrigerator Janis Ccs-850 operating in the 12–320 K range.

## 2.3 Results and Discussion

The diffraction patterns of the samples of stoichiometric mixture of PbO, Fe<sub>2</sub>O<sub>3</sub> and Nb<sub>2</sub>O<sub>5</sub> oxide powders (**I**) before activation (a) and after activation for 5, 10, and 15 min (b)–(d), respectively, are shown in Fig. 2.1. Amorphization process indicated by the broadening of the diffraction reflexes and the initial stage of the formation of perovskite structure of PFN are well seen even after 5 min of activation. After 15 min of activation, only the lines corresponding to the perovskite structure are well seen in the diffraction pattern. It is worth noting that the diffraction pattern of the mixture **I** activated for 15 min using the high-energy planetary-centrifugal ball mill AGO-2 is very similar to the patterns reported in

**Fig. 2.1** Diffraction patterns illustrating the effect of mechanical activation on the stoichiometric mixture of  $\text{PbO}$ ,  $\text{Fe}_2\text{O}_3$  and  $\text{Nb}_2\text{O}_5$  (mixture **I**): **a** initial mixture, **b** after mechanical activation for 5 min, **c** after mechanical activation for 10 min, **d** after mechanical activation for 15 min;  $\blacktriangledown$ — $\text{Nb}_2\text{O}_5$ ;  $+$ — $\text{PbO}$ ;  $\bullet$ — $\text{Fe}_2\text{O}_3$ ;  $*$ —PFN

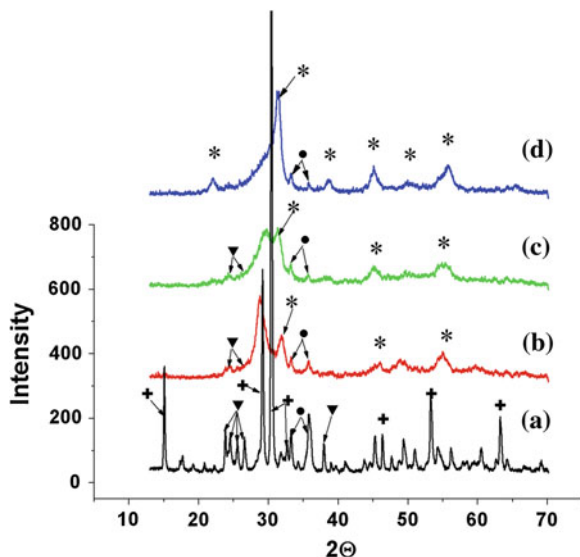
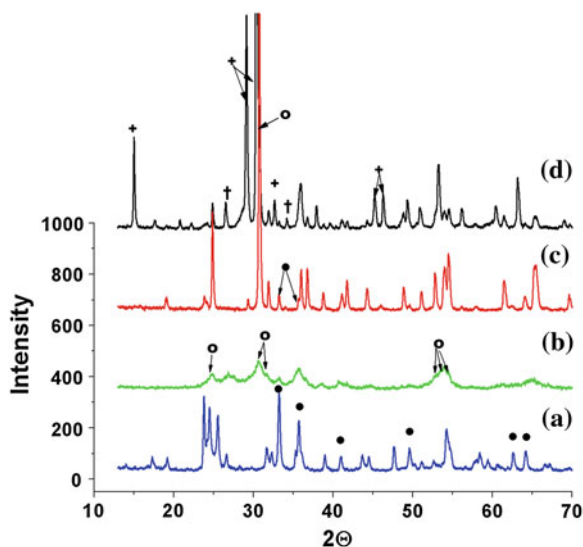


**Fig. 2.2** X-ray diffraction patterns illustrating the stages of the  $\text{FeNbO}_4$  synthesis: **a** initial mixture of  $\text{Fe}_2\text{O}_3$  and  $\text{Nb}_2\text{O}_5$ ,  $\bullet$ — $\text{Fe}_2\text{O}_3$ , other reflections belong to  $\text{Nb}_2\text{O}_5$ ; **b** after mechanical activation for 15 min,  $\circ$ —reflections of  $\text{FeNbO}_4$ ; **c** after annealing at  $1000^\circ\text{C}$ ,  $\bullet$ — $\text{Fe}_2\text{O}_3$ , other reflections belong to  $\text{FeNbO}_4$ ; **d** mixture of  $\text{FeNbO}_4$  and  $\text{PbO}$ ,  $+$ —basic reflections of  $\text{PbO}$ ,  $\dagger$ —basic reflections of  $\text{Pb}_3\text{O}_4$ , other reflections belong to  $\text{FeNbO}_4$



[19, 20] for the same mixtures activated in a shaker mill for 30 h or in a SPEX 8000D vibrating mill for 20 h, respectively.

One can see in Fig. 2.1d that besides the PFN reflexes, there are also two minor reflexes corresponding to  $\text{Fe}_2\text{O}_3$  indicating that the synthesis of PFN is not complete. One can also expect that some amount of  $\text{FeNbO}_4$  is present, because it appears in the activated mixture of  $\text{Fe}_2\text{O}_3$  and  $\text{Nb}_2\text{O}_5$  (Fig. 2.2b). However, due to a considerable widening of reflexes on the diffraction pattern, no  $\text{PbO}$ ,  $\text{Nb}_2\text{O}_5$ , and  $\text{FeNbO}_4$

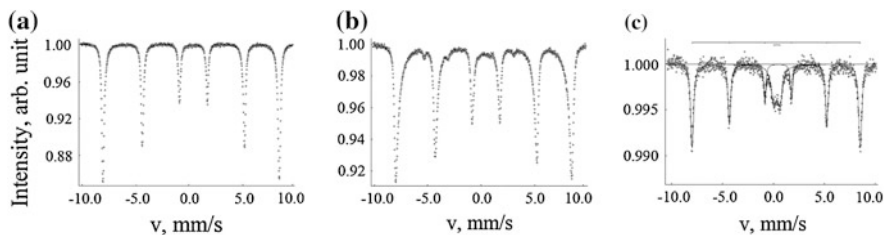


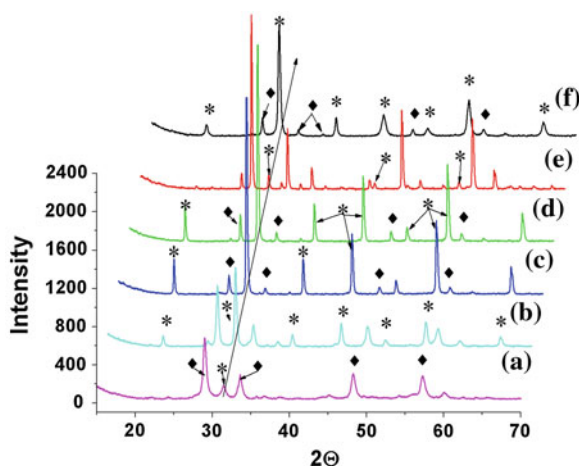
**Fig. 2.3** Room-temperature Mössbauer  $^{57}\text{Fe}$  spectra: **a** initial mixture of  $\text{PbO}$ ,  $\text{Fe}_2\text{O}_3$  and  $\text{Nb}_2\text{O}_5$  (mixture **I**); **b**  $\text{Fe}_2\text{O}_3$  powder after mechanical activation for 15 min; **c** mixture of  $\text{PbO}$ ,  $\text{Fe}_2\text{O}_3$  and  $\text{Nb}_2\text{O}_5$  after mechanical activation for 15 min

reflexes could be unequivocally identified. The mean size of X-ray coherent scattering blocks, estimated using the Scherrer formula for the mixture **I** activated for 15 min, is about 13–20 nm. This value correlates well with the TEM images of the same powder. To have a deeper insight into the phase content of the mechanically activated mixture **I** we studied its room-temperature Mössbauer spectra before and after the activation (Fig. 2.3).

The spectrum of the initial mixture **I** is a sextet corresponding to  $\text{Fe}_2\text{O}_3$  with a hyperfine field of 51.4 T. After mechanical activation of  $\text{Fe}_2\text{O}_3$  powder for 15 min the mean size of X-ray coherent scattering blocks decreased from 35 to 14 nm and the sextet lines have become lower and broader (Fig. 2.3b). After mechanical activation of the initial mixture **I** for 15 min in the room-temperature Mössbauer spectra, besides sextet with a hyperfine field of 51.7 T, there it appears a doublet corresponding to PFN with admixture of  $\text{FeNbO}_4$ . The analysis of Mössbauer spectrum shows that 71.5 % of Fe remains in the  $\text{Fe}_2\text{O}_3$  phase while 27.5 % occurs in the PFN or  $\text{FeNbO}_4$  phase. Similar ratio of the  $\text{Fe}_2\text{O}_3$  and PFN/ $\text{FeNbO}_4$  phases was reported for the stoichiometric mixture of  $\text{PbO}$ ,  $\text{Fe}_2\text{O}_3$  and  $\text{Nb}_2\text{O}_5$  activated in SPEX 8000D vibrating mill for 20 h [20].

The diffraction patterns of the disk samples pressed from the mixture **I** activated for 15 min and annealed for 2 h at different temperatures within 400–1000 °C range are shown in Fig. 2.4. After annealing at 400 °C, the diffraction patterns recorded from this sample exhibit almost no difference as compared to the patterns of unannealed mechanically activated sample (Fig. 2.1d). Only after annealing at 500 °C diffraction patterns start to differ from each other noticeably. One can see in Fig. 2.4a that the growth of  $\text{Pb}_2\text{Fe}_4\text{Nb}_4\text{O}_{21}$  phase is prevailing. After annealing at 600 °C, the PFN phase starts to prevail (Fig. 2.4b), and after annealing at 800 °C its amount becomes much larger (Fig. 2.4c). However, after annealing at 900 °C again the growth of the amount of the  $\text{Pb}_2\text{Fe}_4\text{Nb}_4\text{O}_{21}$  phase starts to dominate (Fig. 2.4d). After annealing at 1000 °C this phase is the major one (Fig. 2.4e) with small reflections of the PFN phase. Even after polishing (Fig. 2.4f) this is not pure PFN, but it contains noticeable amount of  $\text{Pb}_2\text{Fe}_4\text{Nb}_4\text{O}_{21}$ , that is, there is obviously a lack of lead oxide in the samples. Thus it seems that for obtaining the pure perovskite phase using the mechanical activation of the  $\text{PbO}$ ,

**Fig. 2.4** X-ray diffraction patterns of the samples pressed from the mixture of  $\text{PbO}$ ,  $\text{Fe}_2\text{O}_3$  and  $\text{Nb}_2\text{O}_5$  (mixture I) activated for 15 min, after annealing for 2 h at different temperatures: **a** 500 °C, **b** 600 °C, **c** 800 °C, **d** 900 °C, **e** 1000 °C, **f** 1000 °C, polished sample; \*—  $\text{Pb}(\text{Fe}_{0.5}\text{Nb}_{0.5})\text{O}_3$ , ◆—  $\text{Pb}_2\text{Fe}_4\text{Nb}_4\text{O}_{21}$



$\text{Fe}_2\text{O}_3$  and  $\text{Nb}_2\text{O}_5$  oxides one needs to add an excess of  $\text{PbO}$  to the initial stoichiometric mixture.

To synthesize  $\text{FeNbO}_4$  precursor, necessary for obtaining the mixture II, a stoichiometric mixture of  $\text{Fe}_2\text{O}_3$  and  $\text{Nb}_2\text{O}_5$  corresponding to  $\text{FeNbO}_4$  composition (Fig. 2.2a) was activated for 15 min. One can see in Fig. 2.2b that after such activation the reflexes on the diffraction pattern become substantially diffused and chemical interaction between initial components occurs, that is, reflexes corresponding to  $\text{FeNbO}_4$  appear. The powder activated for 15 min was annealed at 1000 °C for 2 h. Iron niobate  $\text{FeNbO}_4$  of monoclinic modification with space group  $\text{P}^*/a$  (no. 13) was formed, but a small amount of unreacted initial  $\text{Fe}_2\text{O}_3$  still remained (Fig. 2.2c).

Then sintered  $\text{FeNbO}_4$  was crumbled and mixed with lead oxide  $\beta\text{-PbO}$ . It is known that the compositions of lead oxides may differ from the stoichiometry. One can see in the diffraction patterns (Fig. 2.1d) that a small amount of red tetragonal  $\beta\text{-Pb}_3\text{O}_4$  is present in yellow rhombic lead oxide  $\beta\text{-PbO}$ .  $\text{FeNbO}_4$  and  $\text{PbO}$  were averaged in a mortar, and then activated in the mill for 15 min. One can see in the diffraction patterns (Fig. 2.5a) that the product formed at once as a result of mechanical activation is single-phase cubic modification of PFN (ASTM code 32-522), space group  $\text{Pm}\bar{3}m$  (no. 221).

During annealing the mechanically activated mixture of  $\text{PbO}$  and  $\text{FeNbO}_4$  within temperature range 400–700 °C, along with PFN, a small amount of the cubic phase  $\text{Pb}_2\text{Fe}_4\text{Nb}_4\text{O}_{21}$  (ASTM code 50-445), space group  $F$ , (no. 0) is formed in the product (Fig. 2.5b). After annealing at 800 °C, the traces of this phase disappear from the diffraction pattern (Fig. 2.5c). The samples annealed at 1000 °C (Fig. 2.5d) exhibit the appearance of magnetoplumbite phase  $\text{PbFe}_{12}\text{O}_{19}$  (ASTM code 84-2046) of hexagonal modification with space group  $\text{P}6_3/\text{mmc}$  (no. 194). The nucleation of this phase starts at a temperature about 900 °C and increases with an increase in annealing temperature. However, this phase is formed predominantly on the surface of the samples. After grinding off the surface layer of

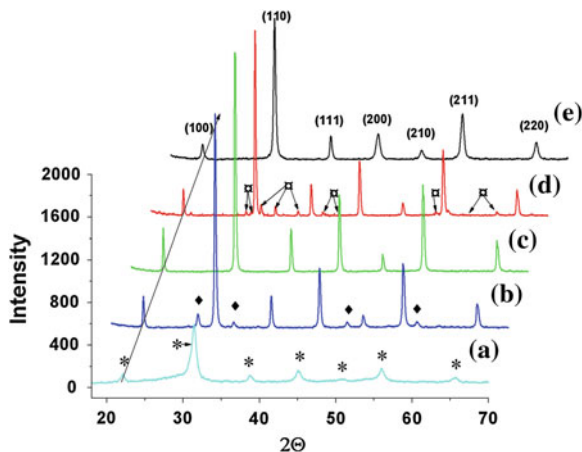


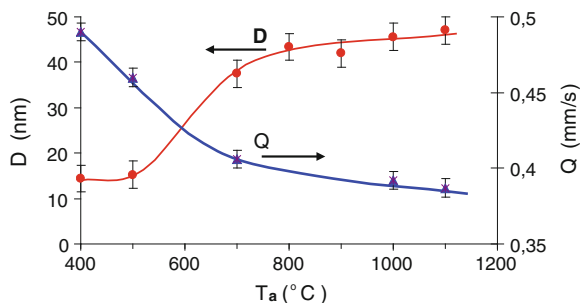
**Fig. 2.5** X-ray diffraction patterns illustrating the effect of annealing on the mechanically activated stoichiometric mixture of PbO and FeNbO<sub>4</sub> (mixture **II**): **a** mixture of PbO and FeNbO<sub>4</sub> mechanically activated for 15 min, **b** after annealing at 700 °C, **c** after annealing at 800 °C (pure PFN), **d** after annealing at 1000 °C, **e** after annealing at 1000 °C and subsequent polishing the sample (pure PFN); ◆—Pb<sub>2</sub>Fe<sub>4</sub>Nb<sub>4</sub>O<sub>21</sub>, ▤—PbFe<sub>12</sub>O<sub>19</sub>, \*—PFN

0.1 mm thick, no traces of this phase are observed in the diffraction patterns (Fig. 2.5e).

After mechanical activation for 15 min, the both mixtures **I** and **II** have rather small mean size  $D$  of the X-ray coherent scattering blocks (10–20 nm) and their X-ray diffraction patterns are diffused. Annealing at 400 °C and 500 °C does not change substantially neither the  $D$  values nor the degree of X-ray diffraction reflexes' diffusion. Annealing at higher temperatures leads to a fast growth of  $D$  values (Fig. 2.6) and sharpening of the X-ray diffraction reflexes with an increase of annealing temperature  $T_a$ . However above approximately 800 °C the  $D(T_a)$  dependence saturates. At room temperature, Mössbauer <sup>57</sup>Fe spectra of all compositions studied appear to be doublets with the isomer shift of  $\approx 0.4$  mm/s (relative to the metallic iron). This value corresponds to the Fe<sup>3+</sup> ions occupying the octahedral sites of the perovskite lattice. The quadrupole splitting in PFN can be caused by the asymmetric environment of the intraoctahedral Fe<sup>3+</sup> ions resulting due to local heterogeneities in the compositional ordering of the Fe<sup>3+</sup> and Nb<sup>5+</sup> ions. This assumption is supported by the fact that, apart from a doublet, the Mössbauer spectrum of highly ordered ternary perovskite PbFe<sub>0.5</sub>Sb<sub>0.5</sub>O<sub>3</sub> contains also a singlet, which is attributed to compositionally ordered regions, whereas the doublet is related to the regions where a long-range ionic order is disturbed [21]. Quadrupole splitting  $Q$  of the Mössbauer <sup>57</sup>Fe doublet spectra of the mechano-activated PFN powders with small (10–20 nm) mean size  $D$  of the X-ray coherent scattering blocks is substantially larger (Fig. 2.6) than that of the single crystal and ceramic samples, in which it is approximately the same ( $\approx 0.4$  mm/s) [22]. As was already mentioned, annealing of the mechanoactivated PFN powders leads to the



**Fig. 2.6** Dependences of the mean size  $D$  of the X-ray coherent scattering blocks and the value of the quadrupole splitting  $Q$  of Mossbauer  $^{57}\text{Fe}$  spectra on the annealing temperature  $T_a$  for the mixture of  $\text{PbO}$  and  $\text{FeNbO}_4$  mechanically activated for 15 min



growth of  $D$  values. This growth is accompanied by gradual decrease of  $Q$  values with increasing the annealing temperature  $T_a$  (Fig. 2.6). At  $T_a > 800$  °C, the quadrupole splitting reaches the level typical of PFN single crystals and ceramics. It is worth noting that large values of quadrupole splitting were reported for the amorphous PFN and they also decreased as a result of annealing leading to the crystallization of the sample [23].

Now, we turn to the temperature dependence of the Mössbauer spectrum. Below  $T_N$ , at cooling, the Mossbauer spectrum transforms from the doublet to a sextet. This transformation is accompanied by a dramatic decrease of the doublet intensity normalized to its value measured at room temperature (Fig. 2.7). The position of the abrupt drop in the temperature dependence of the doublet intensity allows one to obtain the value of  $T_N$  from the Mössbauer experiment. This method was successfully used to determine values of  $T_N$  in several multiferroics and their solid solutions and the results obtained were very similar to the data got by traditional methods such as the magnetization or magnetic susceptibility measurements (see Ref. [22] and references therein). Thus, we have employed this opportunity to detect the temperature of magnetic phase transition in mechanically activated powders with the help of Mössbauer spectroscopy.

Temperature dependencies of the normalized intensity of doublet in Mössbauer spectra for the powders of the stoichiometric mixture of  $\text{PbO}$  and  $\text{FeNbO}_4$  mechanically activated for 15 min and subsequently annealed at different temperatures are shown in Fig. 2.7. The steps on these dependencies correspond to the temperature of magnetic phase transition. For comparison, results for the PFN crystal that was chosen as a reference are shown. One can see that there are two steps on these dependencies for the powders annealed at 400 and 500 °C: one of the steps is at about 40–50 K, and the second one is at higher temperature which depends on annealing temperature  $T_a$  and shifts upward with an increase in  $T_a$ . The powders annealed at 700 °C and at higher temperatures exhibit only one step. The highest temperature of magnetic phase transition possesses the powder annealed at 700 °C. With an increase in  $T_a$  above 700 °C,  $T_N$  starts to decrease, that is, the effect of mechanical activation is annealing, so that for  $T_a = 1000$  and 1100 °C, the  $T_N$  value almost coincides with the one for the PFN crystal.

The low temperature of magnetic phase transition in the unannealed mechanically activated powder is likely to be connected with its «amorphization». The



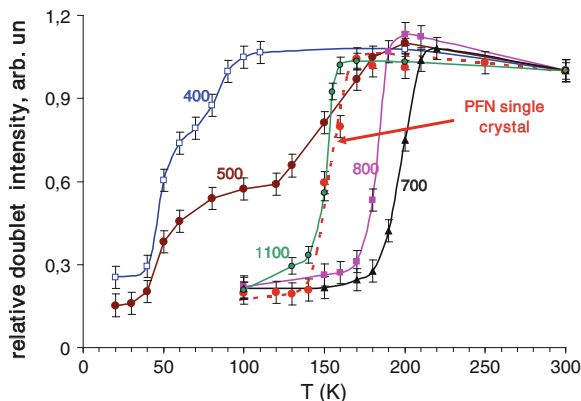


**Fig. 2.7** Dependences of the doublet intensity in the Mössbauer  $^{57}\text{Fe}$  spectrum normalized to its value measured at room temperature for the powders of the stoichiometric mixture of  $\text{PbO}$  and  $\text{FeNbO}_4$  mechanically activated for 15 min and subsequently annealed at different temperatures. Numbers near the curves represent the corresponding annealing temperature. The dashed line shows the data for PFN single crystal

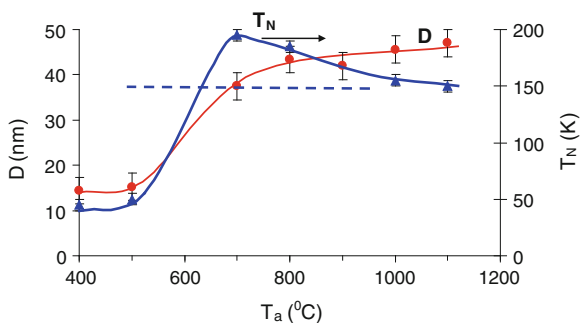
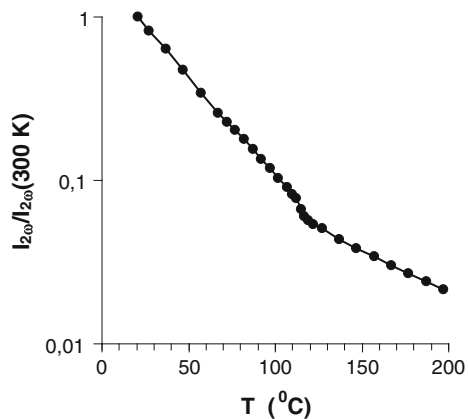


**Fig. 2.8** Dependences of the mean size  $D$  of the X-ray coherent scattering blocks and the Neél temperature  $T_N$  on the annealing temperature  $T_a$  for the mixture of  $\text{PbO}$  and  $\text{FeNbO}_4$  mechanically activated for 15 min. The dashed line marks  $T_N$  value for PFN single crystal

magnetic state in this powder is, most probably, of the spin-glass type, which means that the magnetic order is only short-range. Actually, as this powder gives a normal diffraction pattern, though with broadened lines, this most likely means that the sizes of the regions of the perovskite phase are very small. Annealing is accompanied by an increase in the size of these regions, and the temperature of magnetic transition increases; the formation of long-range antiferromagnetic order is likely to occur. As we suppose, the  $T_N$  value depends also on the degree of iron clustering. Presently it seems that this degree varies comparatively slightly during annealing at temperatures below 700  $^{\circ}\text{C}$ , while at higher  $T_a$  the degree of iron clustering starts to decrease (Fig. 2.8).

**Fig. 2.9** Temperature dependence of the normalized second harmonic generation signal for the powder of PbO and FeNbO<sub>4</sub> stoichiometric mixture mechanically activated for 15 min and subsequently annealed at 700 °C for 2 h



Thus, the present hypothesis explaining the experiment is as follows: for  $T_a < 700$  °C the major factor determining the magnetic phase transition temperature is the coherent length, while for  $T_a > 700$  °C, it is the decrease in the degree of iron clustering with an increase in  $T_a$ .

In order to study if the changes of magnetic phase transition temperature observed for mechanically activated and subsequently annealed PFN powders are accompanied by the changes of the ferroelectric phase transition temperature, we studied the temperature dependence of the second harmonic generation intensity for the powder annealed at 700 °C and showing the largest increase of  $T_N$  as compared to PFN crystal. The experimental setup used was described in details elsewhere [24]. The results obtained are shown in Fig. 2.9. One can see that there is a distinct anomaly in the temperature dependence of the second harmonic generation intensity at about 110 °C. This temperature nicely correlates with the literature data for the ferroelectric-paraelectric phase transition temperature both in single crystals and ceramics of PFN [1, 7, 25]. The character of the dependence of the second harmonic generation intensity on temperature for the PFN powder studied shows some differences as compared to the similar dependencies for BaTiO<sub>3</sub> powders [24, 26]. However it is known that the shape of this curve may be changed crucially by changing the conditions of pressing the powders and their subsequent annealing [26].

## 2.4 Summary

The use of the high-energy planetary-centrifugal ball mill AGO-2 enables one to perform the mechanically activated synthesis of PFN at much shorter time (15 min instead of 20–30 h).

Mössbauer studies have shown that the temperature of magnetic phase transition in PbFe<sub>0.5</sub>Nb<sub>0.5</sub>O<sub>3</sub> powders can be changed by mechanical activation and

subsequent annealing. In particular, the increase by more than 50 K was achieved in the mechanically activated powder of stoichiometric PbO and FeNbO<sub>4</sub> mixture annealed at 700 °C. These results are in line with the model assuming that the temperature of magnetic phase transition in PbFe<sub>0.5</sub>Nb<sub>0.5</sub>O<sub>3</sub> depends substantially on the degree of Fe<sup>3+</sup> and Nb<sup>5+</sup> ions clustering [13]. At the same time the second harmonic generation studies did not reveal any substantial changes of the ferroelectric phase transition temperature in this powder.

**Acknowledgments** This work was partially supported by the Russian Foundation for Basic Research (RFBR) by grants #13-03-00869\_a, #12-08-00887\_a, and the Research Committee of the University of Macau under Research & Development Grant for Chair Professor. Dr. Raevskaya S. I. thanks the Southern Federal University for financial support in fulfillment of this research.

## References

1. W. Kleemann, V.V. Shvartsman, P. Borisov, A. Kania, *Phys. Rev. Lett.* **105**, 257202 (2010)
2. I.P. Rayevsky, M.S. Novikov, L.A. Petrukhnina, O.A. Gubaidulina, A.Ye. Kuimov, M.A. Malitskaya, *Ferroelectrics* **131**, 327 (1992)
3. A.A. Bokov, L.A. Shpak, I.P. Rayevsky, *J. Phys Chem. Solids* **54**, 495 (1993)
4. VYu. Shonov, I.P. Raevski, A.A. Bokov, *Tech. Phys.* **41**, 166 (1996)
5. E.I. Sitalo, YuN Zakharov, A.G. Lutokhin, S.I. Raevskaya, I.P. Raevski, M.S. Panchelyuga, V.V. Titov, L.E. Pustovaya, I.N. Zakharchenko, A.T. Kozakov, A.A. Pavelko, *Ferroelectrics* **389**, 107 (2009)
6. E.I. Sitalo, I.P. Raevski, A.G. Lutokhin, A.V. Blazhevich, S.P. Kubrin, S.I. Raevskaya, YuN Zakharov, M.A. Malitskaya, V.V. Titov, I.N. Zakharchenko, *IEEE Trans. Ultrason. Ferroelectr. Freq. Control* **58**, 1914 (2011)
7. D.A. Sanchez, N. Ortega, A. Kumar, G. Sreenivasulu, R.S. Katiyar, J.F. Scott, D.M. Evans, M. Arredondo-Arechavala, A. Schilling, J.M. Gregg, *J. Appl. Phys.* **113**, 074105 (2013)
8. V.M. Yudin, A.G. Tutov, A.B. Sherman, V.A. Isupov, *Izv. Akad. Nauk SSSR, Ser. Fiz.* **31**(11), 1798 (1967) (in Russian)
9. A.A. Bokov, V.Y. Shonov, I.P. Rayevsky, E.S. Gagarina, M.F. Kupriyanov, *J Phys Condens Matter* **5**, 5491 (1993)
10. I.P. Raevski, S.A. Prosandeev, S.M. Emelyanov, F.I. Savenko, I.N. Zakharchenko, O.A. Bunina, A.S. Bogatin, S.I. Raevskaya, E.S. Gagarina, E.V. Sahkar, L. Jastrabik, *Integr Ferroelectr* **53**, 475 (2003)
11. G.-M. Rotaru, B. Roessli, A. Amato, S.N. Gvasaliya, C. Mudry, S.G. Lushnikov, T.A. Shaplygina, *Phys. Rev. B* **79**, 184430 (2009)
12. V.V. Laguta, J. Rosa, L. Jastrabik, R. Blinc, P. Cevc, B. Zalar, M. Remskar, S.I. Raevskaya, I.P. Raevski, *Mater. Res. Bull.* **45**, 1720 (2010)
13. I.P. Raevski, S.P. Kubrin, S.I. Raevskaya, D.A. Sarychev, S.A. Prosandeev, M.A. Malitskaya, *Phys. Rev. B* **85**, 224412 (2012)
14. V.V. Laguta, M.D. Glinchuk, M. Maryško, R.O. Kuzian, S.A. Prosandeev, S.I. Raevskaya, V.G. Smotrakov, V.V. Eremkin, I.P. Raevski, *Phys. Rev. B* **87**, 064403 (2013)
15. I.P. Raevski, S.P. Kubrin, S.I. Raevskaya, V.V. Titov, D.A. Sarychev, M.A. Malitskaya, I.N. Zakharchenko, S.A. Prosandeev, *Phys. Rev. B* **80**, 024108 (2009)
16. I.P. Raevski, S.P. Kubrin, S.I. Raevskaya, V.V. Titov, S.A. Prosandeev, D.A. Sarychev, M.A. Malitskaya, V.V. Stashenko, I.N. Zakharchenko, *Ferroelectrics* **398**, 16 (2010)
17. E.G. Avvakumov, L.G. Karakchiev, *Chem Sustain Dev* **12**, 287 (2004). (in Russian)

18. L.B. Kong, T.S. Zhang, J. Ma, F. Boey, *Prog. Mater Sci.* **53**, 207 (2008)
19. X.S. Gao, J.M. Xue, J. Wang, T. Yu, Z.X. Shen, *J Am Ceram Soc* **85**(3), 565 (2002)
20. D. Bochenek, G. Dercz, D. Oleszak, *Arch. Metall. Mater.* **56**(4), 1015 (2011)
21. I.P. Raevski, N.M. Olekhovich, A.V. Pushkarev, Y.V. Radyush, S.P. Kubrin, S.I. Raevskaya, M.A. Malitskaya, V.V. Titov, V.V. Stashenko, *Ferroelectrics* **444**, 47 (2013)
22. I.P. Raevski, S.P. Kubrin, S.I. Raevskaya, V.V. Stashenko, D.A. Sarychev, M.A. Malitskaya, M.A. Seredkina, V.G. Smotrakov, I.N. Zakharchenko, V.V. Eremkin, *Ferroelectrics* **373**, 121 (2008)
23. L.N. Korotkov, S.N. Kozhukhar, V.V. Posmet'ev, D.V. Urazov, D.F. Rogovoi, Y.V. Barmin, S.P. Kubrin, S.I. Raevskaya, I.P. Raevskii, *Tech. Phys.* **54**(8), 1147 (2009)
24. A.M. Pugachev, V.I. Kovalevskii, N.V. Surovtsev, S. Kojima, S.A. Prosandeev, I.P. Raevski, S.I. Raevskaya, *Phys. Rev. Lett.* **108**, 247601 (2012)
25. I.P. Raevski, S.P. Kubrin, S.I. Raevskaya, S.A. Prosandeev, M.A. Malitskaya, V.V. Titov, D.A. Sarychev, A.V. Blazhevich, I.N. Zakharchenko, *IEEE Trans. Ultrason. Ferroelectr. Freq. Control* **59**, 1872 (2012)
26. V.I. Kovalevskii, V.K. Malinovskii, A.M. Pugachev, I.P. Raevski, S.I. Raevskaya, P.D. Rudych, N.V. Surovtsev, *Phys. Solid State* **54**(5), 920 (2012)

Advanced Materials

Physics, Mechanics and Applications

Chang, S.-H.; Parinov, I.A.; Topolov, V.Y. (Eds.)

2014, XVIII, 380 p. 221 illus., 40 illus. in color.,

Hardcover

ISBN: 978-3-319-03748-6